



Contents lists available at ScienceDirect

# Bioorganic & Medicinal Chemistry Letters

journal homepage: [www.elsevier.com/locate/bmcl](http://www.elsevier.com/locate/bmcl)

## Synthesis and evaluation of a new series of Neuropeptide S receptor antagonists

Jeffrey Y. Melamed<sup>a,\*</sup>, Amy E. Zartman<sup>a</sup>, Nathan R. Kett<sup>a</sup>, Anthony L. Gotter<sup>b</sup>, Victor N. Uebele<sup>b</sup>, Duane R. Reiss<sup>b</sup>, Cindra L. Condra<sup>b</sup>, Christine Fandozzi<sup>c</sup>, Laura S. Lubbers<sup>b</sup>, Blake A. Rowe<sup>b</sup>, Georgia B. McGaughey<sup>d</sup>, Martin Henault<sup>e</sup>, Rino Stocco<sup>e</sup>, John J. Renger<sup>b</sup>, George D. Hartman<sup>a</sup>, Mark T. Bilodeau<sup>a</sup>, B. Wesley Trotter<sup>f</sup>

<sup>a</sup> Department of Medicinal Chemistry, Merck Research Laboratories, West Point, PA, USA

<sup>b</sup> Department of Neuroscience, Merck Research Laboratories, West Point, PA, USA

<sup>c</sup> Department of Drug Metabolism, Merck Research Laboratories, West Point, PA, USA

<sup>d</sup> Department of Chemistry Modeling and Informatics, Merck Research Laboratories, West Point, PA, USA

<sup>e</sup> In Vitro Sciences Group, Merck Canada, Montreal, Canada

<sup>f</sup> Department of Medicinal Chemistry, Merck Research Laboratories, Boston, MA, USA

### ARTICLE INFO

#### Article history:

Received 8 March 2010

Revised 28 April 2010

Accepted 30 April 2010

Available online 5 May 2010

#### Keyword:

Neuropeptide S receptor

### ABSTRACT

Administration of Neuropeptide S (NPS) has been shown to produce arousal, that is, independent of novelty and to induce wakefulness by suppressing all stages of sleep, as demonstrated by EEG recordings in rat. Medicinal chemistry efforts have identified a quinolinone class of potent NPSR antagonists that readily cross the blood–brain barrier. We detail here optimization efforts resulting in the identification of a potent NPSR antagonist which dose-dependently and specifically inhibited <sup>125</sup>I-NPS binding in the CNS when administered to rats.

© 2010 Elsevier Ltd. All rights reserved.

The Neuropeptide S Receptor (NPSR or GPR154) is a G protein coupled receptor, that is, expressed in regions of the central nervous system that regulate sleep, wake and anxiety.<sup>1,2</sup> NPS is a 20 amino acid peptide, that is, a very potent agonist of NPSR ( $K_d = 0.33$  nM).<sup>2</sup> Central administration of NPS has been shown to produce arousal and induce wakefulness by suppressing all stages of sleep, as demonstrated by EEG recordings in rats.<sup>1</sup> Studies have also shown that the peptide shows anxiety reducing activity.<sup>1</sup> These observations suggest that an NPSR antagonist could represent a novel opportunity for treatment of sleep-related and/or psychological disorders.

Though the de-orphanization of NPSR was reported relatively recently, reports in the patent and medicinal chemistry literature have identified a class of 1,1-diphenyl-hexahydro-oxazolo[3,4-a]pyrazin-3-ones small molecule NPSR antagonists.<sup>3a,b</sup> A representative compound from this series was shown to prevent the effects of ICV-administered NPS in mice, and recently the effects of the compound in animal models of behavior were reported.<sup>3c</sup>

The objective of this effort was to develop tool compounds that are appropriate for assessing the effects of NPSR antagonism in vivo. To achieve this, we required a potent antagonist with sufficient free exposure in the brain to achieve high antagonism in vivo and with minimal off-target activities that could confound

the interpretation of in vivo effects. In this Letter, we describe the optimization of a lead series to achieve a potent, selective NPSR antagonist, that is, well tolerated and demonstrates good occupancy of NPSR in the brain.

An initial high-throughput screening effort led to quinolinone-based lead **1** (Fig. 1). Compound **1** is a potent NPSR antagonist ( $IC_{50} = 18$  nM) but was shown to be a substrate for the P-glycoprotein transporter (P-gp) in vitro. In order to increase the likelihood of compound exposure in the CNS, we set reduction of P-gp susceptibility as a primary goal of initial optimization. Analogs with varied cyclohexylamide substitution showed that the SAR in this region was tight and not likely to afford the required improvements in properties. The basic piperazine functionality of **1** was

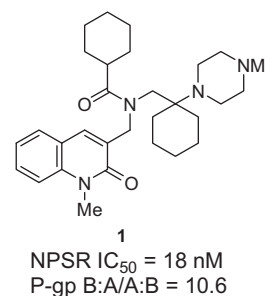
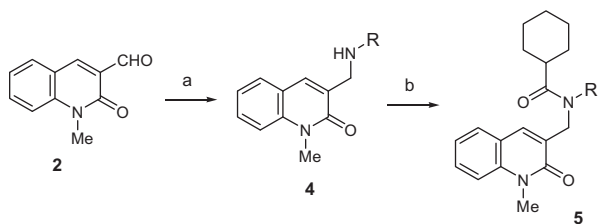


Figure 1. Quinolinone NPSR antagonist.

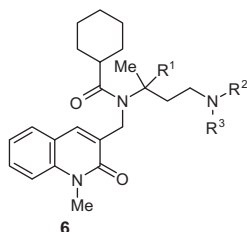
\* Corresponding author at present address: Synthonyx, 3805 Old Easton Rd., Doylestown, PA 18902, USA. Tel.: +1 215 264 2570.

E-mail address: [jmelamed@synthonix.com](mailto:jmelamed@synthonix.com) (J.Y. Melamed).



**Scheme 1.** Reagents: (a)  $\text{NaBH}(\text{OAc})_3$ , amine, DCE; (b) cyclohexanecarbonyl chloride, TEA, DCM.

**Table 1**  
SAR studies of propyl diamine NPSR antagonists



Compound	R <sup>1</sup>	NR <sup>2</sup> R <sup>3</sup>	Human NPSR IC <sub>50</sub> <sup>a</sup> (nM)	B:A/A:B <sup>b</sup>	Papp <sup>c</sup>
<b>6a</b>	H		1577	n.d.	n.d.
<b>6b</b>	H		725	n.d.	n.d.
<b>6c</b>	Me		326	n.d.	n.d.
<b>6d</b>	Me		31	36	25
<b>6e</b>	Me		144	2.0	23

<sup>a</sup> Values represent the numerical average of at least two experiments. Interassay variability was  $\pm 30\%$  (IC<sub>50</sub>, nM).

<sup>b</sup> MDR1 Directional Transport Ratio (B to A)/(A to B). Values represent the average of three experiments and interassay variability was  $\pm 20\%$ .

<sup>c</sup> Passive permeability ( $10^{-6}$  cm/s).

postulated to be a potential contributor to P-gp transport of the compound.<sup>4</sup> However, we found no conservative alterations of this moiety that both preserved potency and substantially reduced P-gp susceptibility.

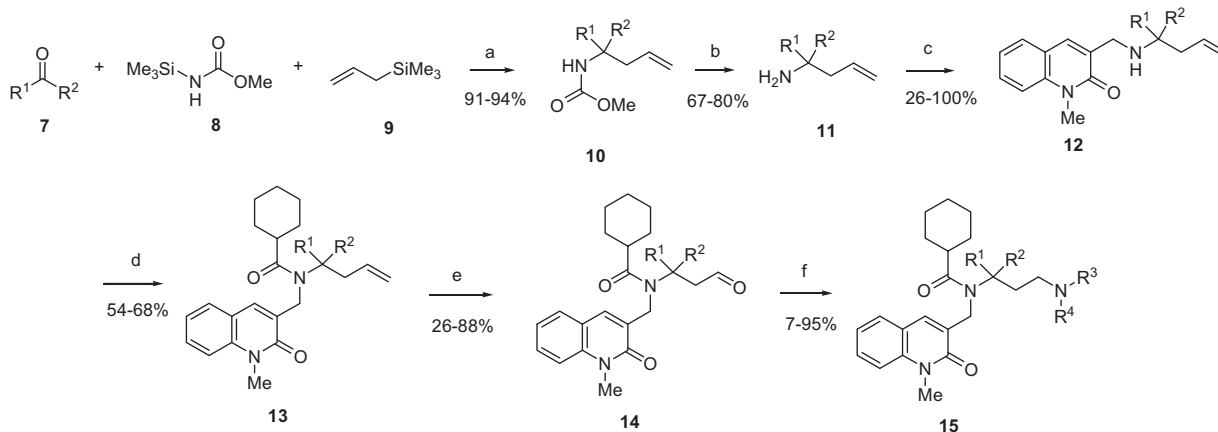
Among the approaches that were attempted to replace the piperazinylcyclohexyl moiety, one ultimately fruitful effort involved computationally evaluating commercial and proprietary amines to select a set of potential replacements for the synthesis of a library. This involved the use of a shape-matching computational algorithm to identify replacements for the entire piperazinylcyclohexylmethyl amine portion of the molecule. This was accomplished by applying a proprietary computational approach called SQW.<sup>5</sup> SQW seeks to maximize volume overlap between a probe molecule or a set of so-called sphere points with a target database using knowledge of chemical typing and shape.

More than 100 amines identified by the shape-matching algorithm were incorporated into the lead series according to Scheme 1. The synthesis begins with the reductive amination of commercially available 1-methyl-2-oxo-1,2-dihydroquinoline-3-carbaldehyde (**2**, Scheme 1) with an amine using sodium triacetoxyborohydride to provide **4**. Unpurified **4** is then treated with cyclohexanecarbonyl chloride and triethylamine to provide **5** in moderate to 28–37% yields over two steps after automated reverse-phase purification.

Evaluation of this set of compounds<sup>6</sup> indicated that the 1,3-propanediamine substructure represented a viable scaffold for non-piperazinecyclohexyl NPSR antagonists (Table 1). Branched analogs (**6a–b**, R = H) were moderately potent. Addition of a methyl group to the propyl linker provided a significant boost in potency (see **6a**, **6b** vs **6c**, **6e**). Replacement of the pyrrolidine in **6c** with a piperidine ring led to **6d**, which provided a 10-fold boost in potency to 31 nM.

However, **6d** remained a P-gp substrate with a B:A/A:B ratio of 36, presumably due in part to the presence of the basic amine. Accordingly, morpholine derivative **6e**, though less potent than **6d**, was not a P-gp substrate (B:A/A:B = 2.0). We therefore targeted further variation of this amine functionality to recover potency while avoiding P-gp susceptibility. To this end, we envisioned a synthetic route that would allow for variation of the amine at the last step of the synthesis and allow alteration of the gem dimethyl moiety. Yokozawa and co-workers have described a three-component coupling procedure for aldehydes, allylsilanes, and an ammonia equivalent that provides compounds of type **10** where R<sup>1</sup> = H and R<sup>2</sup> is a simple aryl or alkyl moiety.<sup>7</sup>

We found that this protocol could be extended to ketones by proper choice of conditions and use of TES–OTf as the Lewis acid



**Scheme 2.** Reagents and conditions: (a) cat. TES–OTf, DCM, 0 °C to rt, 18 h; (b)  $\text{NH}_2\text{NH}_2$ , KOH, ethylene glycol, 200 °C; (c) **2**,  $\text{NaBH}(\text{OAc})_3$ ; (d) cyclohexanecarbonyl chloride, DIEA; (e)  $\text{OsO}_4$ , NMO,  $\text{NaIO}_4$ ; (f)  $\text{HNR}'\text{R}'$ ,  $\text{NaBH}(\text{OAc})_3$ , HOAc, NaOAc.

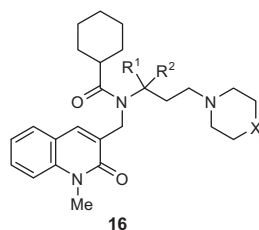
promoter. This procedure provided a rapid synthesis of the appropriate R<sup>1</sup>, R<sup>2</sup> substituted *N*-homoallylcarbamates **10** (Scheme 2), which could be deprotected and then reductively alkylated with **2** to provide the desired amines **12**. Further elaboration provided the key aldehyde intermediates **14**, which could then undergo reductive amination with various primary and secondary amines.

This sequence provided a broad array of amines, of which piperidines and morpholines were preferred. We also found that subtle modifications of substitution in the linker region were effective for enhancing antagonist potency. Ethyl, methyl-substituted compound **16a** (Table 2) showed more than fourfold improvement in potency compared to the dimethyl analog **6d**. The addition of fluorine substituents to the piperidine ring decreased P-gp susceptibility, presumably by lowering the basicity of the amine, but also led

to a significant increase in plasma protein binding. We found that the morpholine derivative **16d** possessed a unique combination of good physical properties and low P-gp susceptibility on this scaffold. Further increasing the size of the geminal alkyl substituents (see di-ethyl analog **16e** and cyclohexyl analog **16f**) decreased activity (Table 2).

The two enantiomers of **16d** were separated using chiral chromatography to give the potent antipode **NPSR-QA1**<sup>8</sup> (NPSR-quinolinone amide **1**), as well as its much less potent enantiomer **16g**. Compound **NPSR-QA1** exhibited potent NPSR antagonism, was not a P-gp substrate, and had a high plasma free fraction (18% in human plasma). Consistent with these data, the compound achieved good brain and CSF levels when dosed to rats. A 30 mg/kg IP dose provided the following tissue levels at 0.5 h: plasma/brain/

**Table 2**  
SAR studies of propyl diamine NPSR antagonists



Compound	R <sup>1</sup>	R <sup>2</sup>	Human NPSR		B:A/A:B <sup>b</sup>	Papp <sup>c</sup>	Prot. Bnd.
			X	IC <sub>50</sub> <sup>a</sup> (nM)			
<b>16a</b> (racemic)	Me	Et	CH <sub>2</sub>	7	43	28	89%
<b>16b</b> (racemic)	Me	Et	CHF	14	2.6	33	n.d.
<b>16c</b> (racemic)	Me	Et	CF <sub>2</sub>	22	1.1	25	97%
<b>16d</b> (racemic)	Me	Et	O	23	0.5	18	91%
<b>16e</b> (racemic)	Et	Et	O	103	n.d.	n.d.	n.d.
<b>16f</b> (racemic)			O	398	n.d.	n.d.	n.d.
<b>NPSR-QA1</b> ( <b>16d</b> enantiomer 1)	Me	Et	O	10	1.7	36	82%
<b>16g</b> ( <b>16d</b> enantiomer 2)	Et	Me	O	785	n.d.	n.d.	n.d.

<sup>a</sup> Values represent the numerical average of at least two experiments. Interassay variability was  $\pm 30\%$  (IC<sub>50</sub>, nM).

<sup>b</sup> MDR1 Directional Transport Ratio (B to A)/(A to B). Values represent the average of three experiments and interassay variability was  $\pm 20\%$ .

<sup>c</sup> Passive permeability ( $10^{-6}$  cm/s).

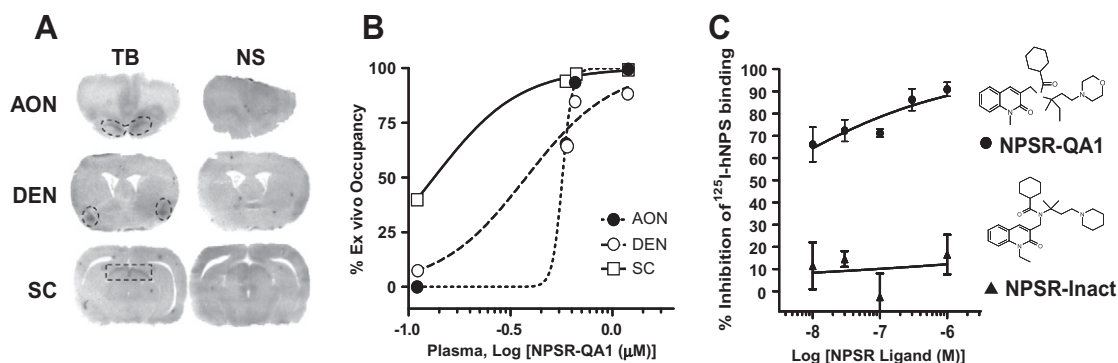


**Figure 2.** **NPSR-QA1** dose-dependently occupied <sup>125</sup>I-hNPS binding sites in discrete regions of the rat brain. (A) Total <sup>125</sup>I-hNPS binding (TB) relative to non-specific binding (NSB) in anterior olfactory nucleus (AON), dorsal endopiriform nucleus (DEN) and superior colliculus (SC). TB in tissue sections from vehicle-treated animals ( $n = 2$ ; 25% HPB cyclodextrin: 75% sterile water, ip) was determined following incubation with 0.5 nM <sup>125</sup>I-hNPS and compared to NSB in adjacent sections incubated with <sup>125</sup>I-hNPS and an excess of 2  $\mu$ M unlabeled hNPS. Areas of interest in the coronal plane of the rat brain are demarcated by dashed lines. (B) Dose-dependent ex vivo occupancy by **NPSR-QA1** in discrete brain regions 30 min after ip dosing ( $n = 4$  rats;  $n = 2$ –3 brain sections/rat). Tissue sections from vehicle- or **NPSR-QA1**-treated animals were incubated with <sup>125</sup>I-hNPS (0.5 nM, 30 min) and mean percent occupancy of **NPSR-QA1** versus plasma concentration of the compound was determined for AON (filled circles, dotted line; IC<sub>50</sub> = 0.57  $\mu$ M;  $R^2 = 1.0$ ), DEN (open circles, dashed line; IC<sub>50</sub> = 0.38  $\mu$ M;  $R^2 = 0.97$ ) and SC (open squares, solid line; IC<sub>50</sub> = 0.13  $\mu$ M;  $R^2 = 0.99$ ) using non-linear regression. (C) **NPSR-QA1**, but not an inactive NPSR ligand, inhibited binding of <sup>125</sup>I-hNPS in SC. In vitro incubation of **NPSR-QA1** (circles) dose-dependently attenuated mean ( $\pm$ SEM) <sup>125</sup>I-hNPS binding in SC (IC<sub>50</sub> = 1.44 nM) of vehicle-treated animals while a structurally similar inactive compound, **NPSR-Inact** (triangles) did not. Total binding was determined by incubating tissue with <sup>125</sup>I-hNPS (0.5 nM, 30 min) in the absence of a NPSR ligand. Non-specific binding of tissue was determined by co-incubation of <sup>125</sup>I-hNPS with 2  $\mu$ M unlabeled hNPS ( $n = 2$ –3 brain sections/concentration).

CSF (nM) = 4344, 1690, 101 and at 2.0 h: plasma/brain/CSF (nM) = 2297, 665, 45. **NPSR-QA1** was tested against a broad panel of receptor and enzyme assays and had no off-target activities with an  $IC_{50} < 10 \mu M$  (170 targets tested at MDS Pharma Services). **NPSR-QA1** showed potent binding to the rat NPSR receptor in in vitro binding displacement studies with an  $EC_{50} = 1.3 nM$ .<sup>9</sup> These data suggest that **NPSR-QA1** is a potent and selective tool for studying the effects of NPSR antagonism in vivo and were supplemented with a study looking at the ability of **NPSR-QA1** to occupy the target when the compound was dosed IP.

The ability of **NPSR-QA1** to penetrate the blood–brain barrier and occupy NPS binding sites was demonstrated in studies examining ex vivo competition for  $^{125}I$ -hNPS binding. Intraperitoneal administration of **NPSR-QA1** (30 mg/kg; 25% HPB cyclodextrin) attenuated  $^{125}I$ -hNPS binding in three different areas of the rat brain including the anterior olfactory nucleus, dorsal endopiriform nucleus and superior colliculus (Fig. 2A and B). Specificity for this binding was substantiated in experiments in which in vitro pre-incubation of brain sections with **NPSR-QA1** blocked  $^{125}I$ -hNPS binding in a concentration-dependent manner, while a structurally similar inactive compound (**NPSR-Inact**,  $EC_{50}$  for binding displacement on the rat receptor =  $1400 nM$ <sup>9</sup>) did not (Fig. 2C).

In summary, a new series of NPSR antagonists has been developed. A potent, highly selective and CNS penetrant antagonist, **NPSR-QA1**, has been identified. This compound has been shown to provide high occupancy of NPSR after IP dosing. Thus, **NPSR-QA1** represents a useful pharmacologic agent for further study of the effects of central NPSR antagonism in vivo.

## References and notes

1. Xu, Y.-L.; Reinscheid, R. K.; Huitron-Resendiz, S.; Clark, S. D.; Wang, Z.; Lin, S. H.; Brucher, F. A.; Zeng, J.; Ly, N. K.; Henriksen, S. J.; Lecea, L.; Civelli, O. *Neuron* **2004**, *43*, 487.
2. Xu, Y.-L.; Gall, C. M.; Jackson, V. R.; Civelli, O.; Reinscheid, R. K. *J. Comp. Neurol.* **2007**, *500*, 84.
3. (a) Zhang, Y.; Gilmour, B. P.; Navarro, H. A.; Runyon, S. P. *Bioorg. Med. Chem. Lett.* **2008**, *18*, 4064; (b) Okamura, N.; Habay, S. A.; Zeng, J.; Chamberlin, A. R.; Reinscheid, R. K. *J. Pharmacol. Exp. Ther.* **2008**, *325*, 893; (c) Ruzza, C.; Rizzi, A.; Trapella, C.; Pela', M.; Camarda, V.; Ruggieri, V.; Filafarro, M.; Cifani, C.; Reinscheid, R. K.; Vitale, G.; Ciccocioppo, R.; Salvadori, S.; Guerrini, R.; Calo', G. *Peptides*, in press.
4. Cox, C. D.; Breslin, M. J.; Whitman, D. B.; Coleman, P. J.; Garbaccio, R. M.; Fraley, M. E.; Zrada, M. M.; Buser, C. A.; Walsh, E. S.; Hamilton, K.; Lobell, R. B.; Tao, W.; Abrams, M. T.; South, V. J.; Huber, H. E.; Kohl, N. E.; Hartman, G. D. *Bioorg. Med. Chem. Lett.* **2007**, *17*, 2697.
5. Miller, M. D.; Sheridan, R. P.; Kearsley, S. L. *J. Med. Chem.* **1999**, *42*, 1505.
6. A dual sequence fluorometric imaging plate reader (FLIPR)  $Ca^{2+}$  mobilization assay was used to evaluate compounds for agonist and antagonist activity on the Neuropeptide S receptor expressed on recombinant CHOK1 cells plated in 384-well PDL coated plates 24 h prior to experiment (15Kcells/well/20  $\mu l$ ). Following washing with buffer and loading with Fluo4AM dye for 1 h at 37 °C in 5%  $CO_2$ , cell plates were placed in the FLIPR and incubated with titrated compounds for 4 min during sequence 1 data collection. In sequence 2, an EC80 of human NPS was added to the assay plates and data collected for another 4 min. Percent stimulatory activity (sequence 1) or inhibition (sequence 2) was calculated relative to  $Ca^{2+}$  mobilization in NPS stimulated control wells (EC100 or EC80 NPS). Compound potencies were determined from plots of concentration response curves using 4p logistical fits and reported as means  $\pm$  SD of multiple determinations.
7. Niimi, L.; Serita, K.; Hiraoka, S.; Yokozawa, T. *Tetrahedron Lett.* **2000**, *41*, 7075.
8. Single enantiomer (faster eluting peak) was obtained via chiral HPLC. Absolute stereochemistry has not been determined.
9. Binding experiments employed radiolabeled compound **1**. Radiolabeling of **1** was accomplished by tri-tritiation of the N-Me quinolinone moiety by alkylation of the un-methylated quinolinone.